

Determination of the multiple-scattering correction factor and its cross-sensitivity to scattering for different AE33 Aethalometer filter tapes: A multi-instrumental approach

Jesús Yus-Díez^{1,2}, Vera Bernardoni³, Griša Močnik^{4,5}, Andrés Alastuey¹, Davide Ciniglia³, Matic Ivančič⁶, Xavier Querol¹, Noemí Perez¹, Cristina Reche¹, Martin Rigler⁶, Sara Valentini³, Roberta Vecchi³, and Marco Pandolfi¹

¹Institute of Environmental Assessment and Water Research (IDAEA-CSIC), C/Jordi Girona 18-26, 08034, Barcelona, Spain

²Departament de Física Aplicada - Meteorologia, Universitat de Barcelona, C/Martí i Franquès, 1., 08028, Barcelona, Spain

³Dipartimento di Fisica “A. Pontremoli”, Università degli Studi di Milano & INFN-Milan, via Celoria 16, 20133 Milano, Italy

⁴Center for Atmospheric Research, University of Nova Gorica, Vipavska 11c, SI-5270 Ajdovščina, Slovenia.

⁵Department of Condensed Matter Physics, Jozef Stefan Institute, Jamova 39, SI-1000 Ljubljana, Slovenia

⁶Aerosol d.o.o., Ljubljana, Slovenia

Correspondence: jesus.yus@idaea.csic.es

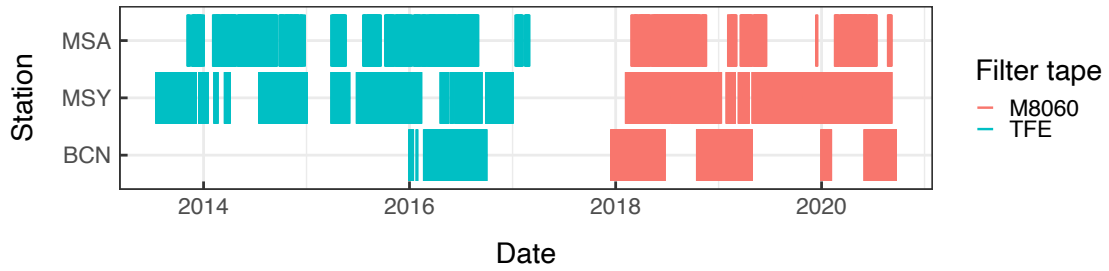


Figure S1. Multiple scattering parameter (C) availability for both M8060 and TFE filter tape at BCN, MSY and MSA measurement supersites.

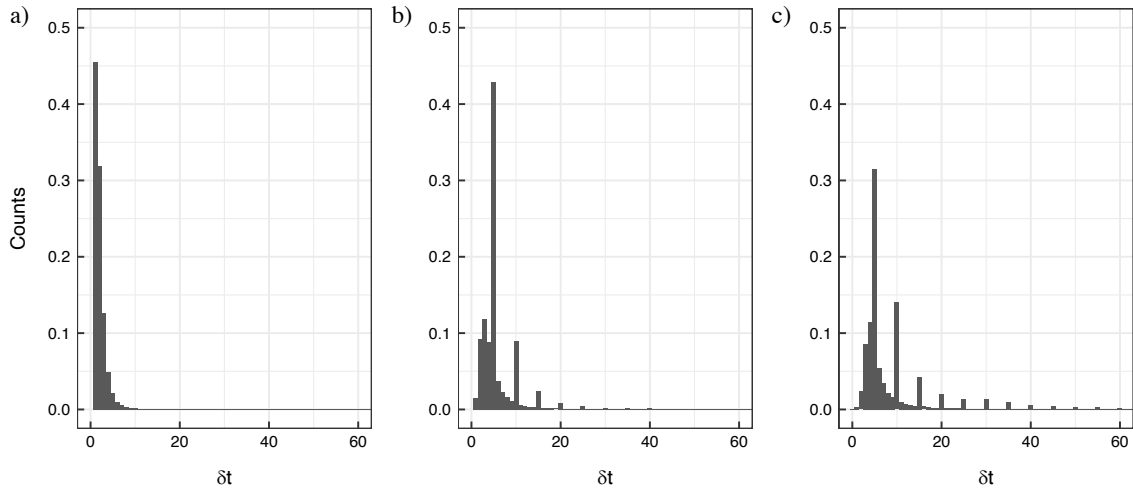


Figure S2. Normalized count distribution of the measurement timestamp, δt in minutes for a) BCN, b) MSY, and c) MSA. Time measurement resolution was set to 1 min when possible, in b) and c) the 5 min spikes are due to a measurement time resolution of 5 min during a certain period of time.

C

	<i>Filter type</i>	DJF	MAM	JJA	SON
BCN	<i>TFE</i>	2.21	2.24	2.31	2.41
	<i>M8060</i>	2.47	2.39	2.33	2.56
MSY	<i>TFE</i>	2.30	2.15	2.42	2.34
	<i>M8060</i>	2.19	2.16	2.31	2.24
MSA	<i>TFE</i>	2.14	2.47	2.35	2.37
	<i>M8060</i>	2.37	2.31	2.74	2.63

Table S1. Median values of the multiple scattering factor (C) for each measurement station and for the two different filter types: TFE-coated glass and M8060 filter tape for the 4 seasons: winter (DJF), spring (MAM), summer (JJA) and autumn (SON).

	$C_{PP_UniMI}(\lambda)$						
	370 nm	470 nm	520 nm	590 nm	660 nm	880 nm	950 nm
<i>BCN</i>	3.36	3.26	3.22	3.24	3.21	3.19	3.31
<i>MSY</i>	2.68	2.67	2.72	2.77	2.79	2.62	6.67
<i>MSA</i>	3.47	3.48	3.58	3.71	3.87	4.05	4.03

Table S2. Multiple scattering factor (C) at each AE33 measuring wavelength obtained using the absorption coefficient from the PP_UniMI polar photometer for BCN, MSY and MSA measurement supersites.

	$C_{PaM}(\lambda)$						
	370 nm	470 nm	520 nm	590 nm	660 nm	880 nm	950 nm
<i>BCN</i>	2.82	2.78	2.75	2.73	2.72	2.69	2.83
<i>MSY</i>	2.32	2.33	2.42	2.46	2.47	2.26	2.32
<i>MSA</i>	2.82	2.85	2.91	3.03	3.09	3.22	3.24

Table S3. Multiple scattering factor (C) at each AE33 measuring wavelength obtained using the absorption coefficient from the PP_UniMI polar photometer working as MAAP (PaM) for BCN, MSY and MSA measurement supersites.

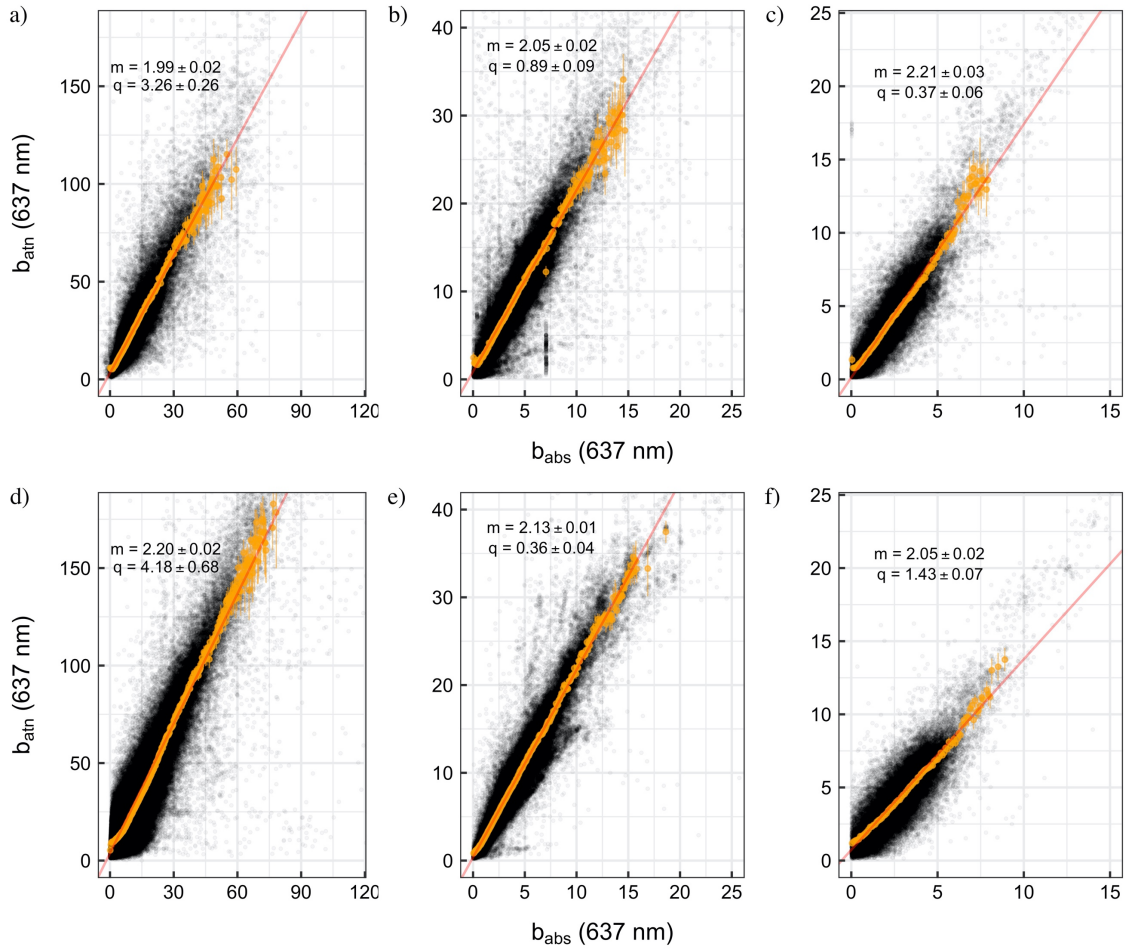


Figure S3. Scatter-plot of the binned AE33 attenuation coefficient (b_{atm} (637 nm)) vs MAAP absorption coefficient b_{abs} (637 nm)) where the slope of the Deming regression, m , represents the multiple-scattering parameter C , and q is the intercept of the regression, for the TFE-coated glass filter tape (upper panels) and M8060 filter tape (lower panels) for BCN (a,d), MSY (b,e) and MSA (c,f). The non-zero intercept, q , is indicative of the additional signal due to the cross-sensitivity to scattering of particles within the filter.

	AAE	
	C_{const}	$C(\lambda)$
BCN	1.19 ± 0.15	1.17 ± 0.15
MSY	1.27 ± 0.12	1.25 ± 0.12
MSA	1.19 ± 0.07	1.35 ± 0.07

Table S4. Mean values of the absorption Ångström exponent (AAE) for the sensitivity analysis performed in Fig. 3 on the AAE obtained using a wavelength-dependent C ($C(\lambda)$) in comparison with an AAE obtained using a constant C (C_{const}) parameter.

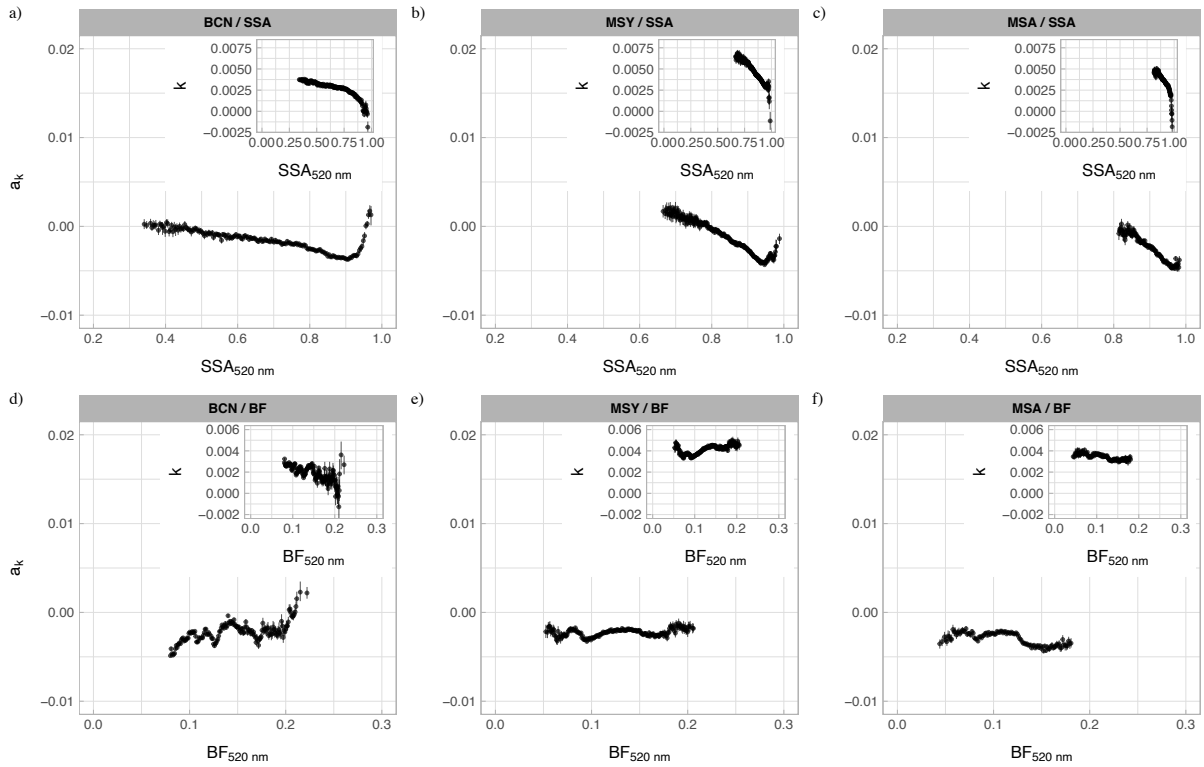


Figure S4. Relationship between the slope of the factor loading k (a_k ; i.e. the slope between k and the wavelength) and single-scattering albedo ($SSA_{520 \text{ nm}}$) and the backscattered fraction ($BF_{520 \text{ nm}}$) at 520 nm at BCN, MSY and MSA. Inset graphs show the dependency of k vs. SSA and BF at 520 nm at the three sites.

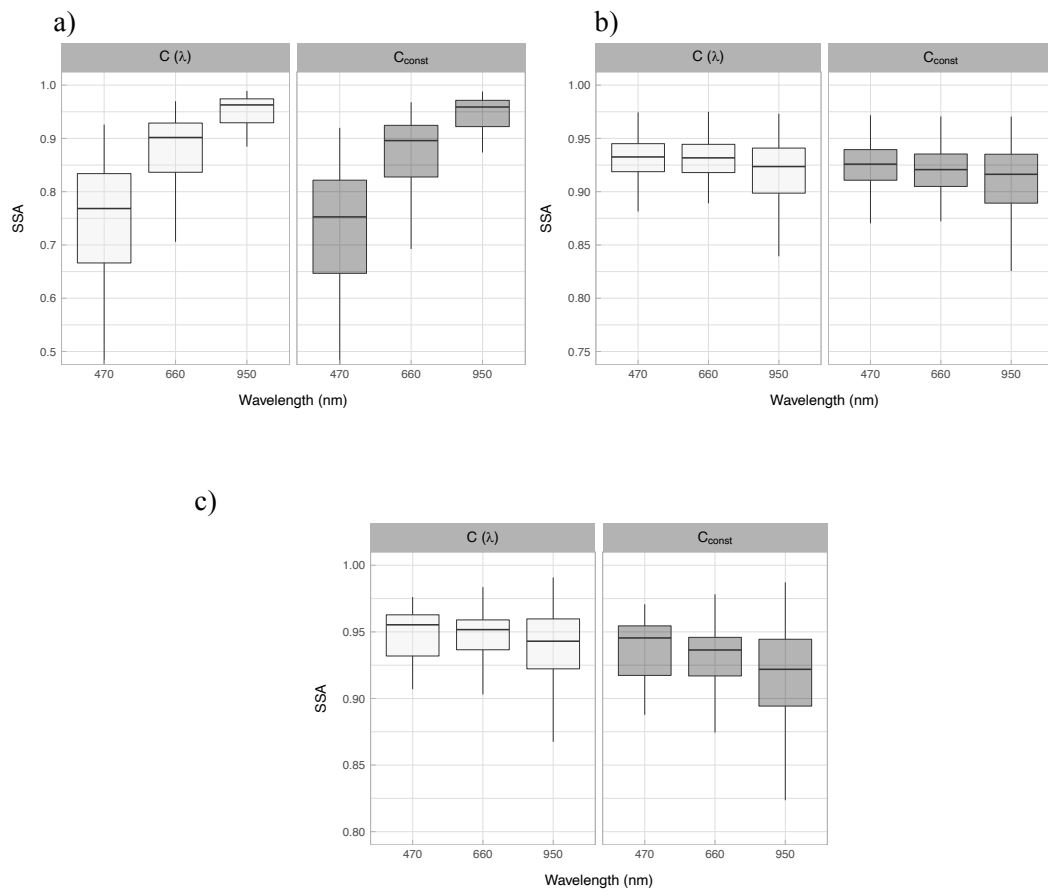


Figure S5. Sensitivity analysis of the single scattering albedo (SSA) on the wavelength-dependent C ($C(\lambda)$) in comparison with an SSA at 3 wavelengths (470, 660 and 950 nm) obtained using a constant C parameter (C_{const}) for a) BCN, b) MSY and c) MSA measurement stations.

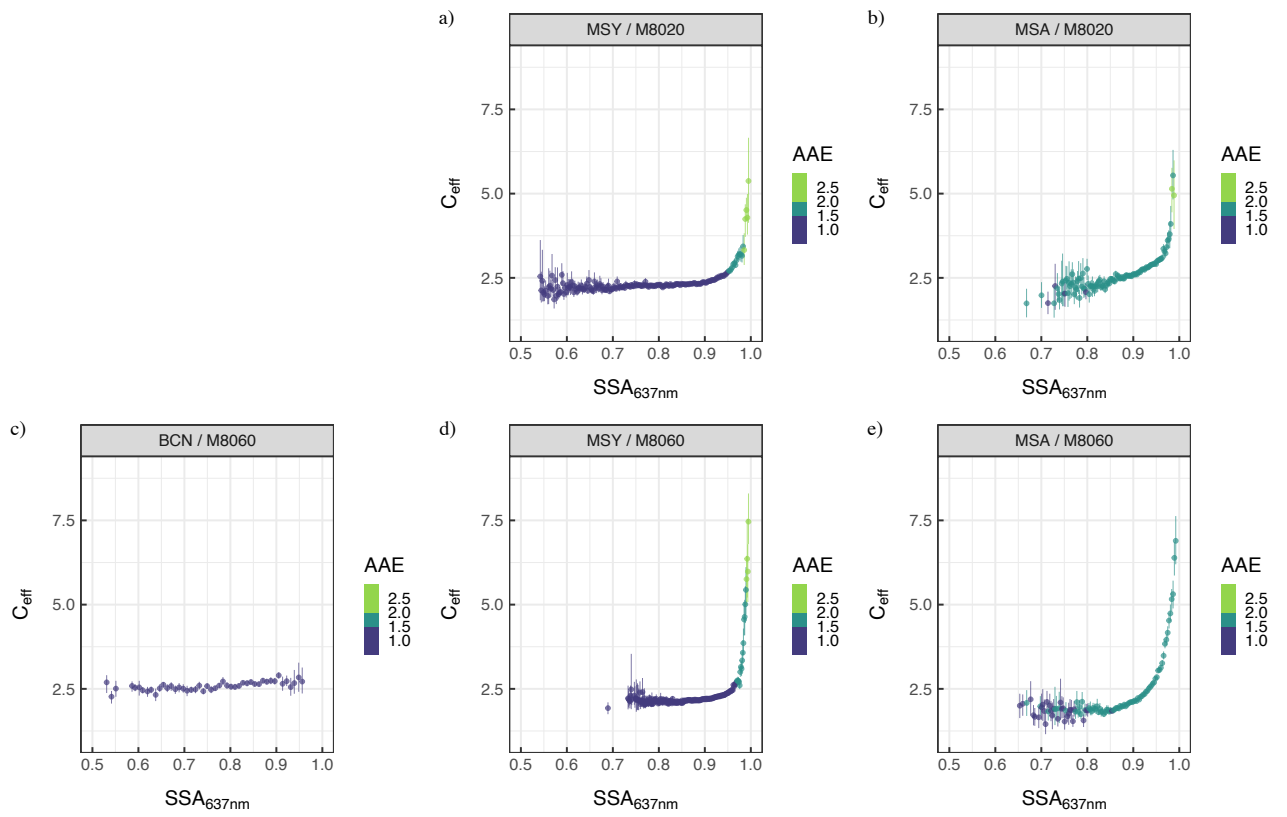


Figure S6. Multiple scattering parameter (C) dependence on the single scattering albedo (SSA) for the TFE-coated glass (upper panel) and the M8060 filter tape (lower panel) at: BCN (c), MSY (a,d) and MSA (b,e) measurement supersites as a function of the absorption Ångström exponent (AAE).

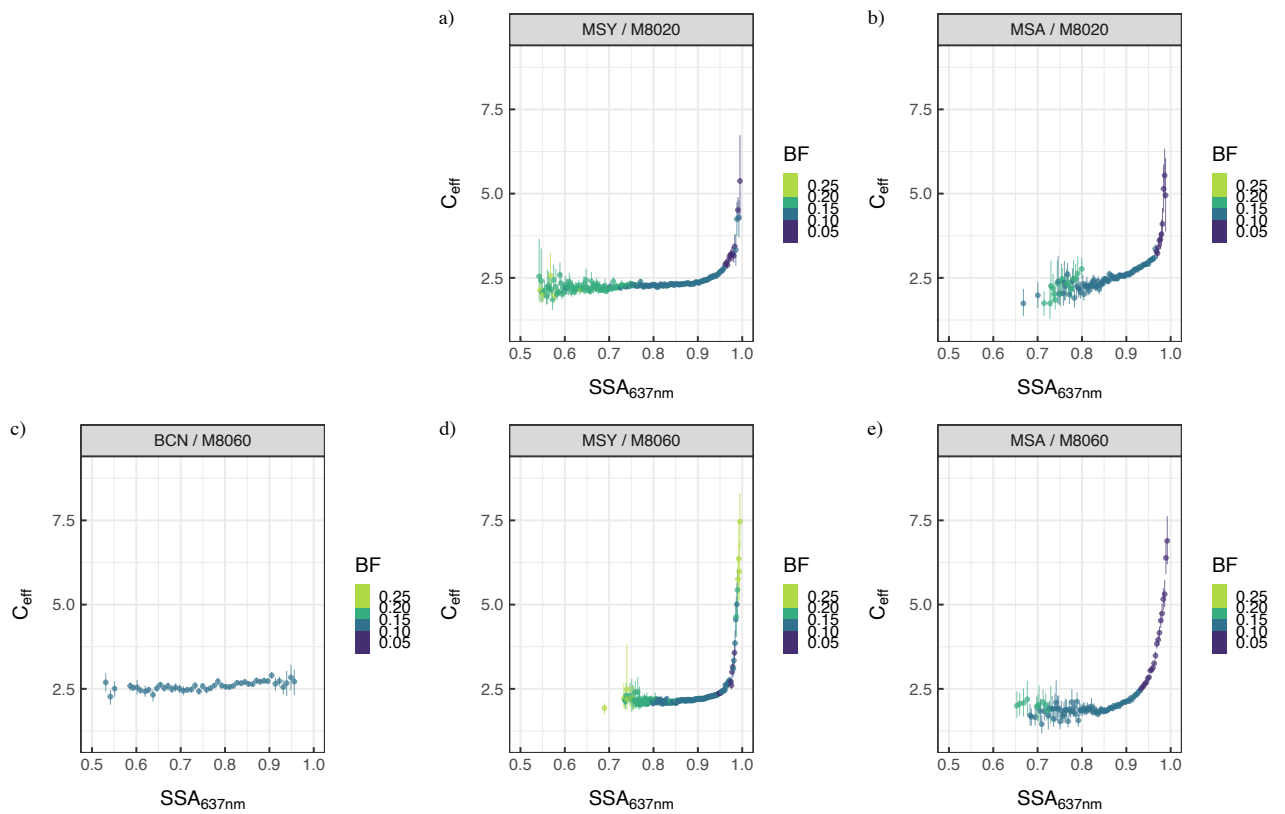


Figure S7. Multiple scattering parameter (C) dependence on the single scattering albedo (SSA) for the TFE-coated glass (upper panel) and the M8060 filter tape (lower panel) at: BCN (c), MSY (a,d) and MSA (b,e) measurement supersites as a function of the backscattered fraction at (BF).

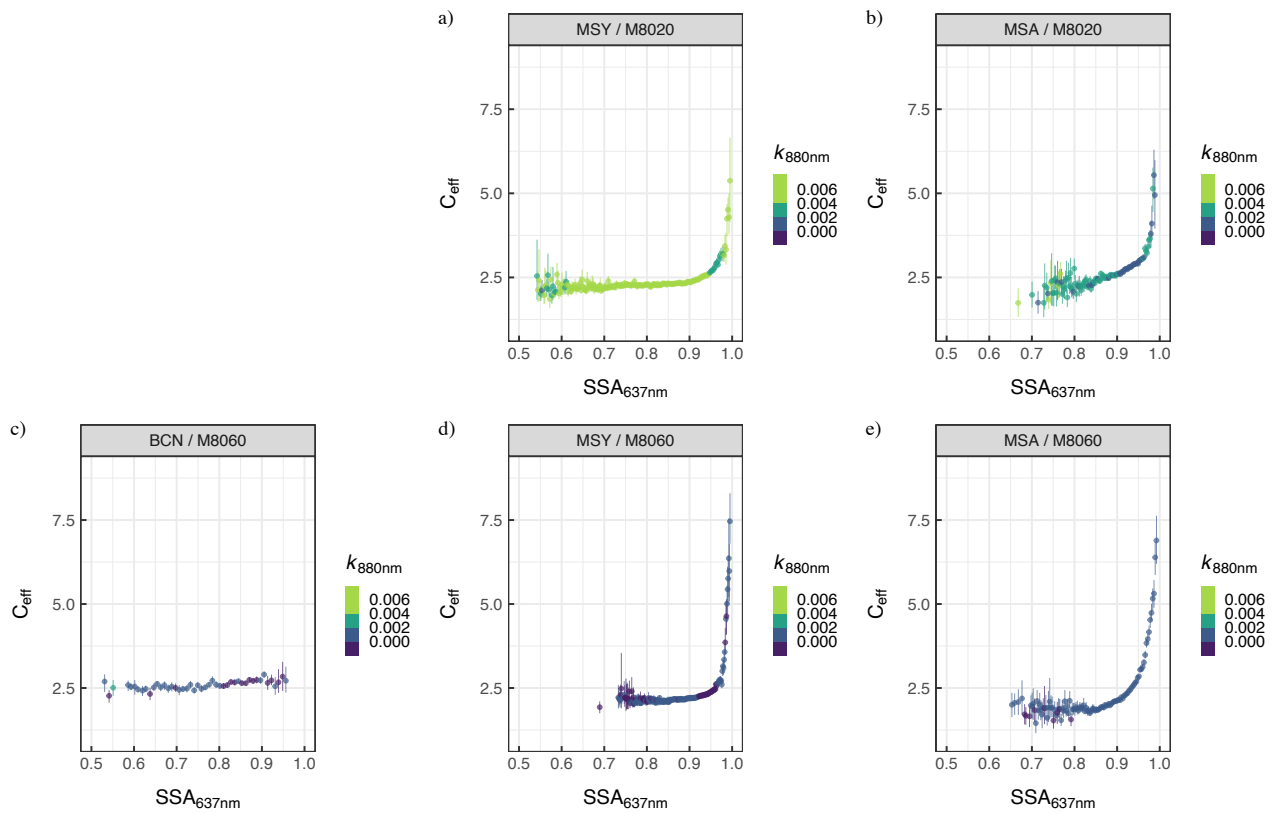


Figure S8. Multiple scattering parameter (C) dependence on the single scattering albedo (SSA) for the TFE-coated glass (upper panel) and the M8060 filter tape (lower panel) at: BCN (c), MSY (a,d) and MSA (b,e) measurement supersites as a function of the factor loading parameter at 880 nm ($k_{880\text{nm}}$).

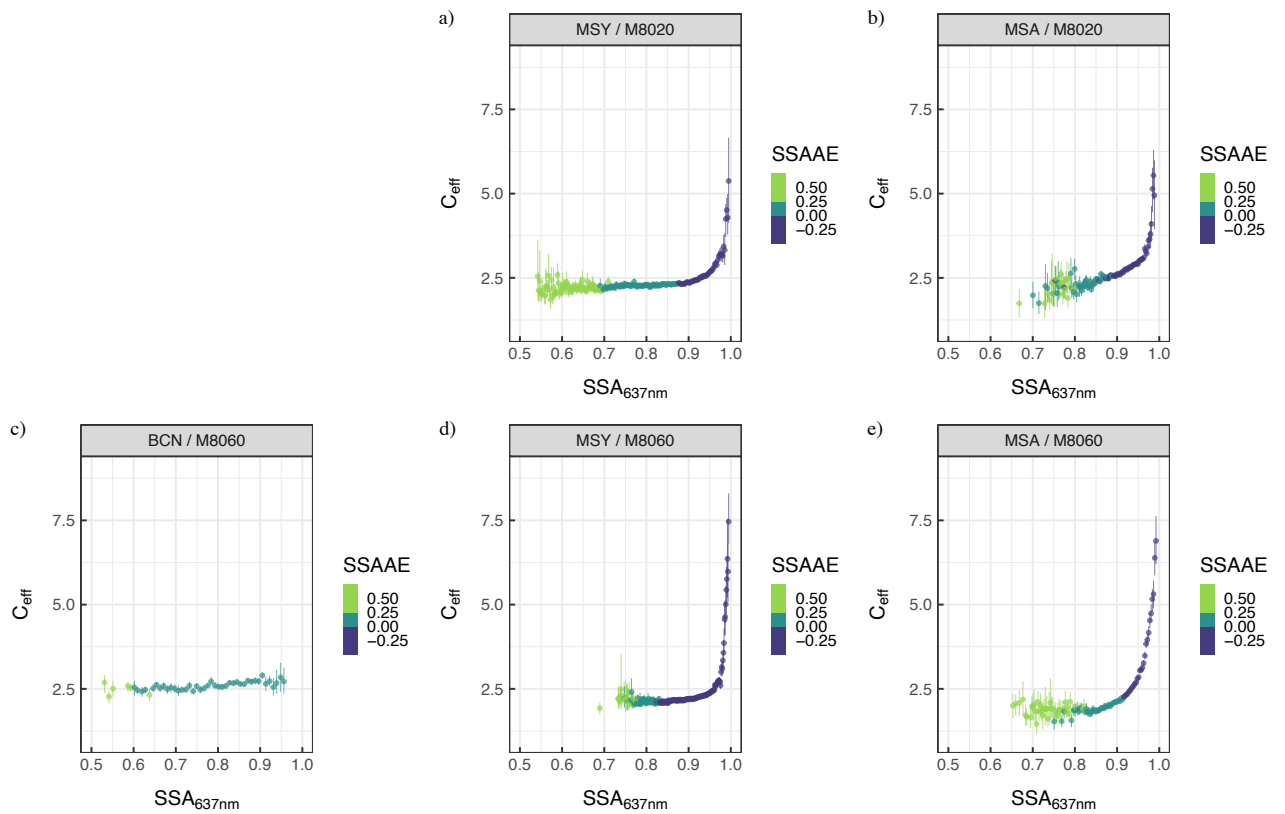


Figure S9. Multiple scattering parameter (C) dependence on the single scattering albedo (SSA) for the TFE-coated glass (upper panel) and the M8060 filter tape (lower panel) at: BCN (c), MSY (a,d) and MSA (b,e) measurement supersites as a function of the single-scattering albedo Ångström exponent (SSAAE).